Research Article

Received: 16 December 2011 Revised: 27 February 2012 Accepted: 28 February 2012 Published online in Wiley Online Library: 22 June 2012

(wileyonlinelibrary.com) DOI 10.1002/pi.4282

Tribological properties of ethylene–propylene–diene rubber + polypropylene + thermal-shock-resistant ceramic composites

Witold Brostow,[a]* Tea Datashvili[a] and James Geodakyan[b]

Abstract

This work is part of a program on composites used in thermoelectric devices. Tribological properties of dynamic vulcanizate blends of polypropylene and ethylene-propylene-diene rubber filled with 5 wt% of microscale powder have been studied. The microscale thermal-shock-resistant ceramic filler contains α-Al_2O_3, mullite ($3Al_2O_3 \cdot 2SiO_2$ or $2Al_2O_3SiO_2$), β-spodumene glass-ceramic and aluminium titanate. We found that our ceramic particles are abrasive; they cause strong abrasion of softer steel ball surfaces during dry sliding friction. To overcome the difficulty of particle dispersion and adhesion, the filler was modified through grafting using three types of organic molecules. Dry sliding friction was measured using four types of counter-surfaces: tungsten carbide, Si_3N_2, 302 steel and 440 steel. Thermoplastic vulcanizate filled with neat ceramic powder shows the lowest friction compared to composites containing the same but surface-treated powder. We introduce a 'bump' model to explain the tribological responses of our composites. 'Naked' or untreated ceramic particles protrude from the polymer surface and cause a decrease of the contact area compared to neat polymer. The ball partner surface has only a small contact area with the bumps. As contact surface area decreases, so does friction and the amount of heat generated during sliding friction testing. Chemical coupling of the ceramic to the matrix smoothens the bumps and increases the contact surface, giving a parallel increase in friction.

Keywords: polymer composite; thermal-shock-resistant ceramic; filler adhesion; filler modification; abrasion; friction

INTRODUCTION

Thermoelectric (TE) generators are devices which convert heat (temperature differences) directly into electrical energy using a phenomenon called the Seebeck effect (discovered in 1821 by the Estonian–German physicist Thomas Johann Seebeck). Automotive TE generators have been proposed to recover usable energy from automobile waste heat – a technology not yet implemented. There is also TE refrigeration based on the Peltier effect (discovered by Jean Peltier after Seebeck's discovery) creating a heat flux at the junction of two different types of conductors connected to a battery. This effect has been used in camping and portable coolers and for cooling electronic components and small instruments. Both TE generators and TE coolers seem to have bright futures[1] – provided their efficiencies can be much increased.

The most often used TE materials are based on bismuth and tellurium. As noted before,[2] TE cooler or generator assemblies also involve polymers, ceramics and other metals. The objective of the work presented here was a study of polymer + ceramic composites for potential TE applications. Since TE devices are subjected to large temperature cycling, we used a thermal-shock-resistant ceramic filler. Specifically, we have already studied thermophysical and mechanical properties of dynamic vulcanizate blends of polypropylene (PP) and ethylene–propylene–diene rubber (EPDM) filled with 5 wt% microscale ceramic powder.[3] Namely, dynamic vulcanization of PP + EPDM polymers turns such a combination into a thermoplastic vulcanizate (TPV). The ceramic surfaces were modified to increase adhesion of the filler to the matrix composites. Materials containing unmodified as well as modified ceramic were investigated. It turned out that brittleness (B) defined in 2006[4] and connected to some other properties[5–7] decreases with surface modification of the ceramic.[3] Ceramic particles are known to be abrasive. Therefore, we have now determined abrasion/wear properties and dynamic friction of the same materials as well as studied composite surfaces using SEM. There have been various studies of tribological properties of polymer-based materials (PBMs)[8–31] but to our knowledge not of PBMs containing high-temperature ceramics. To some extent, the

* *Correspondence to: Witold Brostow, Laboratory of Advanced Polymers and Optimized Materials (LAPOM), Department of Materials Science and Engineering and Department of Physics, University of North Texas, 3940 North Elm Street, Denton, TX 76207, USA. E-mail: brostow@unt.edu*

a *Laboratory of Advanced Polymers and Optimized Materials (LAPOM), Department of Materials Science and Engineering and Department of Physics, University of North Texas, 3940 North Elm Street, Denton, TX 76207, USA*

b *Scientific Research and Production Enterprise of Materials Science, 17 Charents Street, 0025 Yerevan, Armenia*

present paper continues earlier work on the effects of crosslinking agents on the tribological behavior of TPVs.[32]

EXPERIMENTAL

Materials

EPDM samples were received as a gift from Dow Chemical Company. PP pellets were supplied by Huntsman Co. The thermal-shock-resistant ceramic powder contained corundum (α-Al_2O_3), mullite ($3Al_2O_3 \cdot 2SiO_2$), the eutectic of both (the summary formula is thus close to $2Al_2O_3SiO_2$), modified β-spodumene (with negative thermal expansivity) and stabilized aluminium titanate. The ceramic was made by interaction of the minerals in air atmosphere at 1550 °C for 5 h. Then wet pressing with a water + ethanol mixture was applied in a circular-type mill followed by drying. The ceramic had a density $\rho = 3.60$ g cm^{-3}, open porosity of 0.46% and total porosity of 20.0%; the average volumetric thermal expansivity from 20 to 700 °C was $\alpha = 2.5 \times 10^{-6}$ K^{-1}. The ceramic was tested in multiple thermal cycling and found to retain its stability up to 1400 °C. High-magnification SEM images[3] showed that the ceramic particles had approximately rectangular shapes with an average width of *ca* 7 μm and a length between 10 and 30 μm.

Silane coupling agent (SCA 989; 3-methacryloxypropyltrimethoxysilane (MPS)) and titanate coupling agent (Lica 12; neopentyl(diallyl)oxytri(dioctyl)phosphato titanate) were received as gifts from Struktol Company of America and Kenrich Petrochemicals Inc., respectively. Dicumyl peroxide, ethanol and stearic acid came from Sigma Chemicals Co. The reagents were analytically pure and were used as received.

Blending and sample preparation

Dynamic vulcanization was done by melt mixing in a CW Brabender D-52 Preparation Station with addition of dicumyl peroxide. EPDM was softened at 160 °C for 2 min with a mixing speed of 60 rpm. Then we added an equal weight of PP. After addition of PP, blending continued for a further 2 min. Then the polymer matrix was filled with 5.0 wt% thermal-shock-resistant ceramic. Directly after 2 min of mixing, 1.0 wt% curing agent was added (the amount of peroxide was calculated on the basis of EPDM + PP weight). Temperature and mixing speed of the process were increased and kept for 2 min at 190 °C and 90 rpm. Three different types of coupling agents (CAs) were used to modify the ceramic powder. Thus, materials including TPV + ceramic, PP + ceramic and EPDM + ceramic were prepared.

These blends were pelletized and molded in an AB-100 injection molding machine (AB Machinery, Montreal, Quebec, Canada) at 185 °C under an injection pressure of 830 kPa.

Characterization techniques

Environmental scanning electron microscopy (ESEM)

Micrographs of the samples were taken using an FEI Quanta ESEM instrument. Small fraction of the samples were cut and/or fractured in liquid nitrogen, mounted on a copper stub and coated with a thin layer of gold to avoid electrostatic charging during examination.

Surface images of the samples were obtained using a Nikon Eclipse ME 600 microscope.

Friction and wear testing

Dynamic friction was determined using a Nanovea pin-on-disc tribometer from Micro Photonics Inc. Silicon nitride (Si_3N_2), tungsten carbide (WC), 302 steel and 440 steel balls made by Salem Specialty Balls were used. A new 3.2 mm diameter ball was used for each test. The tests were performed under the following conditions: temperature, 20±2 °C; speed, 100 rpm; radius, 2.0 mm; load, 1.0 and 5.0 N; number of revolutions, 5000.

Areas of wear tracks were measured with a Veeco Dektak 150 profilometer with a 12.5 μm radius stylus tip. The applied force was 1.0 mg and the scan rate was 0.033 μm s^{-1}. All samples were cleaned with high-pressure air and alcohol before testing to remove any debris from the surface.

FRICTION AND WEAR RESULTS

As mentioned above, tribology tests were performed using four types of counter-surfaces: WC, Si_3N_2, 302 steel and 440 steel. The results are presented in Fig. 1, which shows the lowest value of dynamic friction for PP + ceramic while the highest is for EPDM + ceramic. All the samples rapidly reach the steady friction value in an early stage of the test; only the friction of the EPDM + ceramic blend increases by 0.05–0.1 after 20 min of the test. For all counter-surfaces, friction curves of the TPV and its composites fall between those of the PP + ceramic and EPDM + ceramic samples. Average dynamic friction values are presented in Fig. 2.

Vickers hardness ($h_{Vickers}$) of the pins decreases in the following order: Si_3N_4 ($h_{Vickers} = 1600$) > WC ($h_{Vickers} = 1300$) > 440 steel ($h_{Vickers} = 279$) > 302 steel ($h_{Vickers} = 166$). Friction increases slightly with the hardness of the ball material. We note that for WC balls the TVP + ceramic + stearic acid system exhibits lower friction than the systems of TVP + ceramic + either of the two CAs. Stearic acid is able to migrate to the composite surface during molding and can act there as a lubricant. Tribology data do not provide a clear correlation between friction and ball type; however, friction trends are the same in all cases. TPV filled with neat ceramic powder shows lower friction compared to composites containing surface-treated powder.

Morphological observations may explain the tribological response of the composites. We infer from ESEM micrographs (Fig. 3) that the CAs do favor a better polymer–filler interaction due to modification of the surface of the ceramic powder with polymerizable organic groups.[3] Wetting of the particles by the polymer matrix is clearly improves after modification, making the sharp parts of the ceramic particles less noticeable. ESEM observations are consistent with our 'bump' model – anticipated earlier[32] and which now will be explained. Without a CA, irregularly shaped ceramic particles protrude upwards from the surface. The partner surface of the ball has only a small contact area with the bumps. With CAs, ceramic particles are well coated with polymer matrix due to improved adhesion and wetting ability. What was a sharp bump now acquires a smoother shape similar to a drop of liquid on a well-wetting surface. The contact surface area increases – and so does friction. We recall that surface energy is related to both friction and scratch resistance.[33] The lowest value of friction for all partner surfaces is seen for PP + ceramic; since PP is relatively hard, ceramic particles provide effective bumps. The highest friction values also for all partner surfaces are seen for EPDM + ceramic. Since EPDM is soft, the ceramic particles do not protrude from the surface and the bump mechanism is inoperative. Thus friction determination and ESEM results are explained by a single model. Our model is an example of the applicability of a general

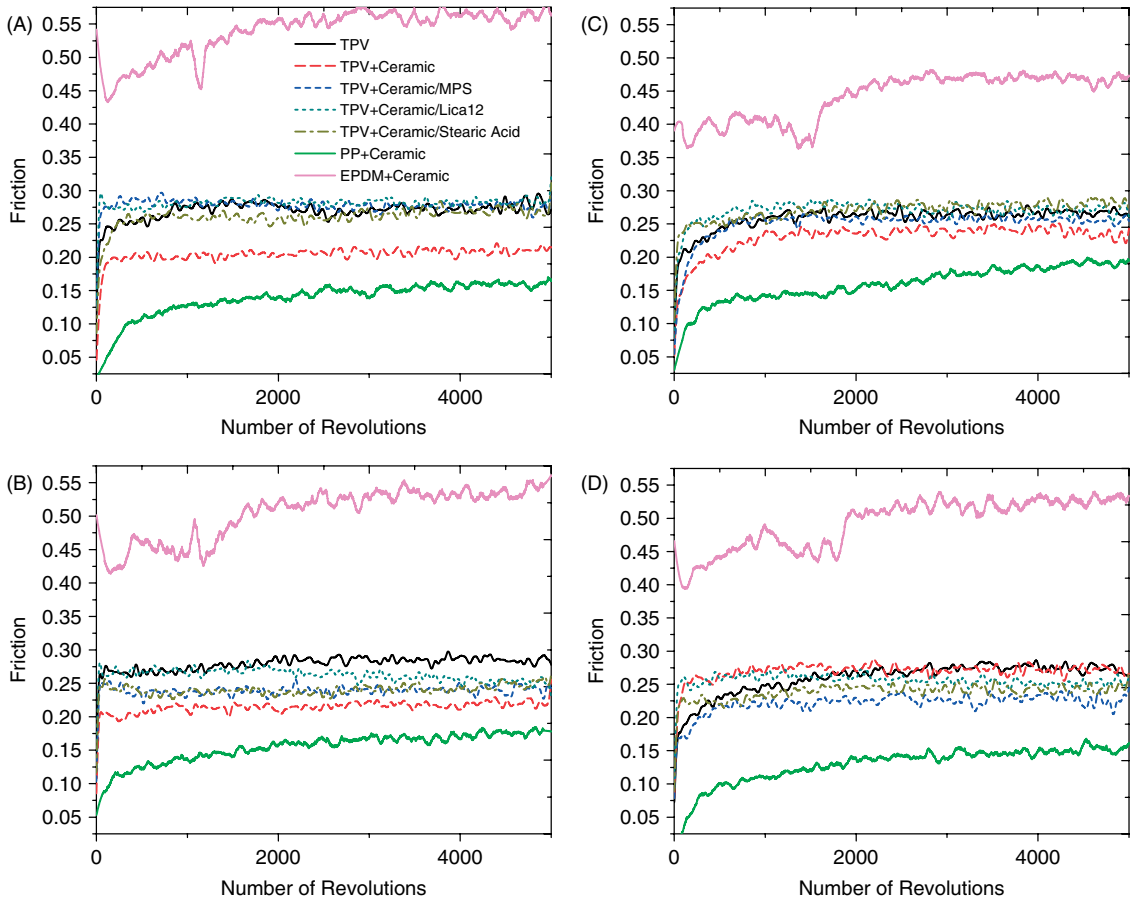

Figure 1. Friction: (A) WC, (B) Si_3N_4, (C) 302 steel and (D) 440 steel balls (key applies to all figure parts).

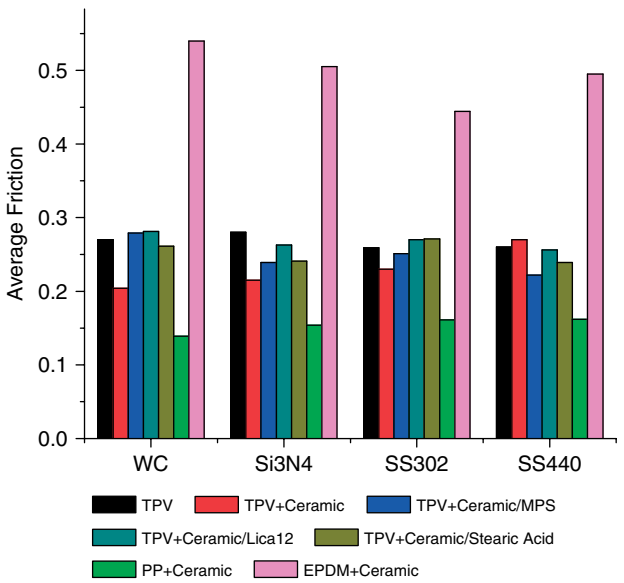

Figure 2. Average friction.

statement made by Desai and Kapral:[34] formation of structures is often controlled by interfaces, interfacial curvatures and defects.

The morphology of the wear tracks shows the same behavior. Unlike modified samples, sharp ceramic particles are easily noticeable inside the wear track of the TPV + ceramic sample (Fig. 4(A)) – which should have significant effects on the contact area and overall tribological performance.

In order to observe removal of materials from TPV and TPV + ceramic surfaces we used a dual focused ion beam (FIB)/SEM system.[35] It combines a Ga^+ ion beam column with high-resolution field emission SEM. The dual beam was run at 52° stage tilt. TPV and TPV + ceramic were milled with a 0.5 nA Ga^+ ion beam current at an accelerating voltage of 30 kV. The inner region of the cross-sectional area was polished (cleaned) with a lower beam current of 50 pA. The depth of the milling specimen was *ca* 2 µm. For both samples milling was done under the same conditions, but due to 'melting damage' it was challenging to apply the Ga^+ ion beam on the TPV sample. In order to decrease sample damage and maintain the same milling conditions, a platinum layer was deposited on the surface of TPV prior to milling (Fig. 5(A)).

Direct comparisons between material removal through ion beam milling and dry sliding friction are not typically made. However, the FIB/SEM image in Fig. 5(B) shows ceramic bumps inside the milled area of TPV + ceramic sample that are similar to sharp ceramic particles detected earlier inside the wear track of TPV + ceramic sample (Fig. 4).

We also examined used ball surfaces after dry sliding tests (Fig. 6). We see that WC and Si_3N_4 balls are resistant to instantaneous deformation while the situation is the reverse for the steel balls. The contact surfaces of the steel balls are damaged during friction with the composites, whereas the same ball surfaces remain unchanged after contact with TPV – known to be a relatively soft material.[36] The results can be explained

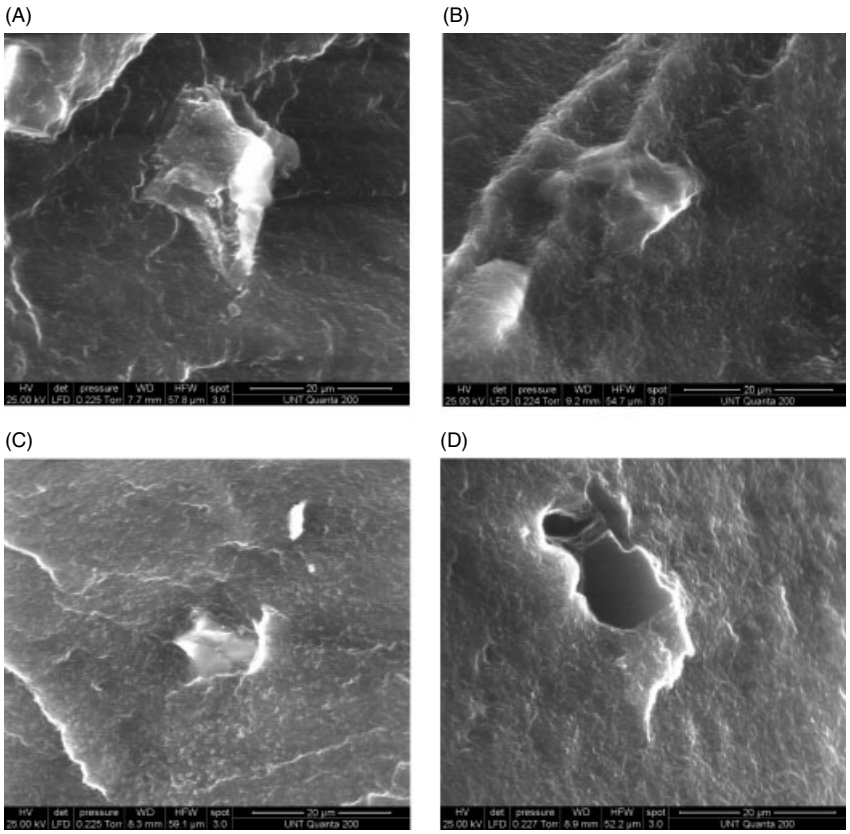

Figure 3. ESEM micrographs: (A) TPV + ceramic; (B) TPV + ceramic/MPS; (C) TPV + ceramic/Lica 12; (D) TPV + ceramic/stearic acid.

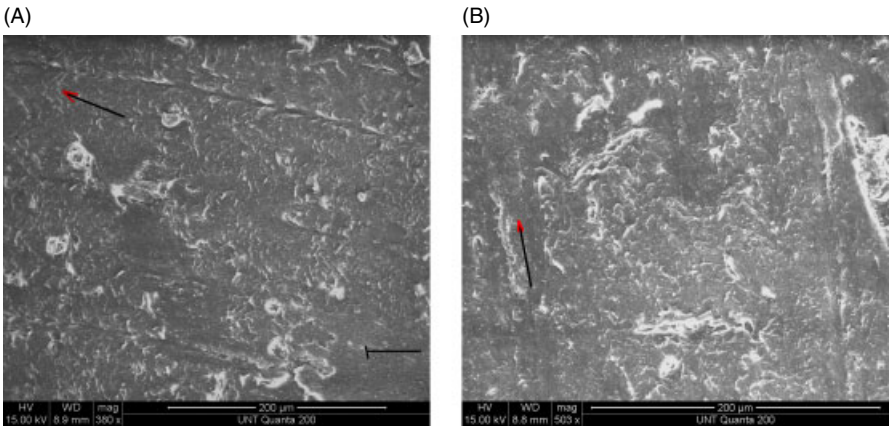

Figure 4. ESEM micrographs of wear track using steel ball: (A) TPV + ceramic; (B) TPV + ceramic/MPS.

in terms of two-body abrasive wear. The hard ceramic particles display abrasive behavior and cause deformation of the softer steel ball surfaces. After friction with TPV + ceramic we find damaged area of 800 to 1000 µm in size with deep scratched lines on it, while worn surfaces of the balls had a size of 600–700 µm after tests with TPV + ceramic/CAs. Clearly, CA mitigates the abrasion of the ceramic powder. As expected, friction behavior of the composites as well as ball deformation depends on the contact materials; the tests were done using 5.0 N normal force. The higher abrasive character of TPV + ceramic composite can also lead to three-body abrasion. A similar phenomenon was reported by Dec and coworkers.[37]

Three-body abrasion is known to take place when hard abrasive particles or wear debris are introduced into a sliding system either as environmental contaminants or as products of two-body abrasion. Abrasive behavior of wear debris generally occurs by plowing, cutting and cracking mechanisms, as discussed by the tribology group of Homel.[25] Apparently the ceramic particles are pulled out from the TPV + ceramic sample due to insufficient adhesion between the components. Those particles act as a third-body abrasive and generate steel particles during friction testing.

ESEM images of TVP and TPV + ceramic surfaces (Figs 7(A) and (B)) show the formation of steel debris after dry sliding friction with 440 steel and 302 steel balls. The resulting steel particles

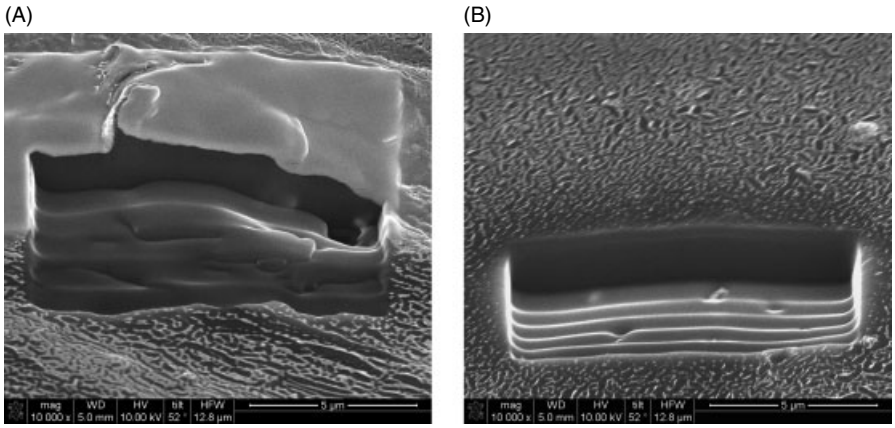

Figure 5. FIB/SEM micrographs: (A) TPV; (B) TPV + ceramic.

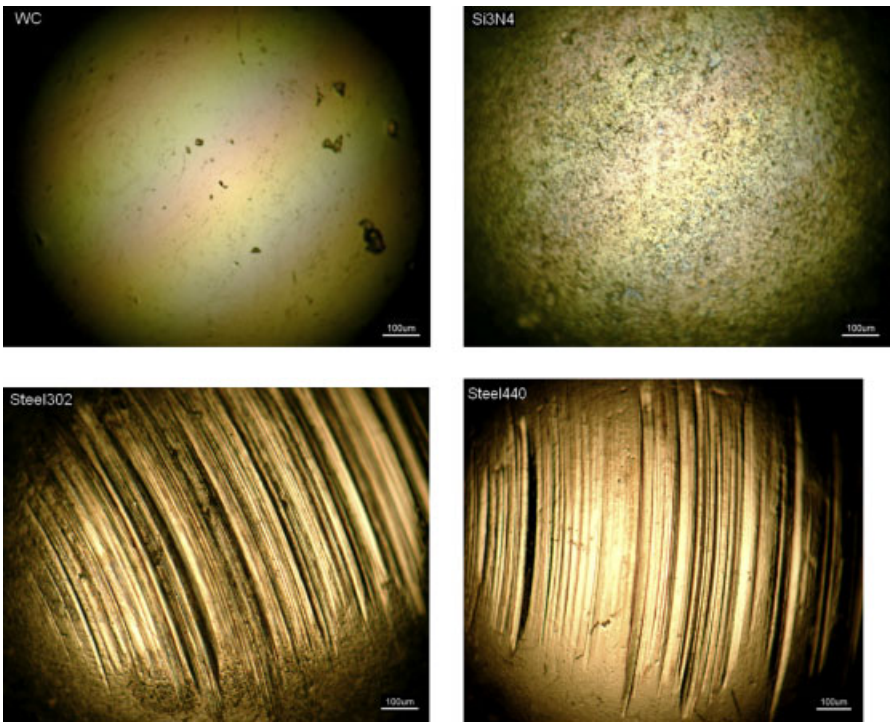

Figure 6. WC, Si_3N_4, 302 steel and 440 steel ball surfaces after friction with TPV + ceramic.

form regions of approximately 200 μm in size inside the wear track (Fig. 7(C)) of the sample. Apart from the abrasive nature of the filler, we do not see significant effects of powder content on TPV matrix deformation during sliding friction. However, from high-resolution ESEM images of wear tracks, TPV + ceramic matrix appears dense and smooth compared to neat TPV which shows non-uniform matrix deformation with fiber-like stretched regions and plastic debris on it. Polymer deformation observed in the absence of filler may be caused by variations in thermal stability and viscosity properties of the samples.

Let us return to the steel ball surfaces. Optical observations of used ball surfaces provide some indications of particle distribution inside the TPV matrix. For example, the materials filled with modified powder have 'drawn' uniform and shallow lines on ball surfaces while TPV + unmodified ceramic causes more aggressive ball deformation with deeper scratches. 'Fingerprints of the filler' on the surface of the steel balls show more homogeneous distribution of modified ceramic particles in the TPV matrix compared to the unmodified powder.

Additional tests were performed to verify our assumption about steel ball surface deformation and to eliminate other possible explanations. Namely, two more EPDM + ceramic and PP + ceramic blends were prepared to study the influence of the matrix on tribological behavior. Moreover, pin-on-disc tests were performed using a lower 1.0 N load. The resulting surfaces are shown in Fig. 8. We find that the milder test conditions (1.0 N instead of 5.0 N) do not change the ball surface deformation tendency. Scratches on the surfaces of the steel balls still appear. There is less surface damage, but the abrasive nature of the ceramic powder is manifested again (Fig. 9).

In contrast to TPV- and EPDM-based composites, smaller steel ball deformations are seen for the PP + ceramic blend. These

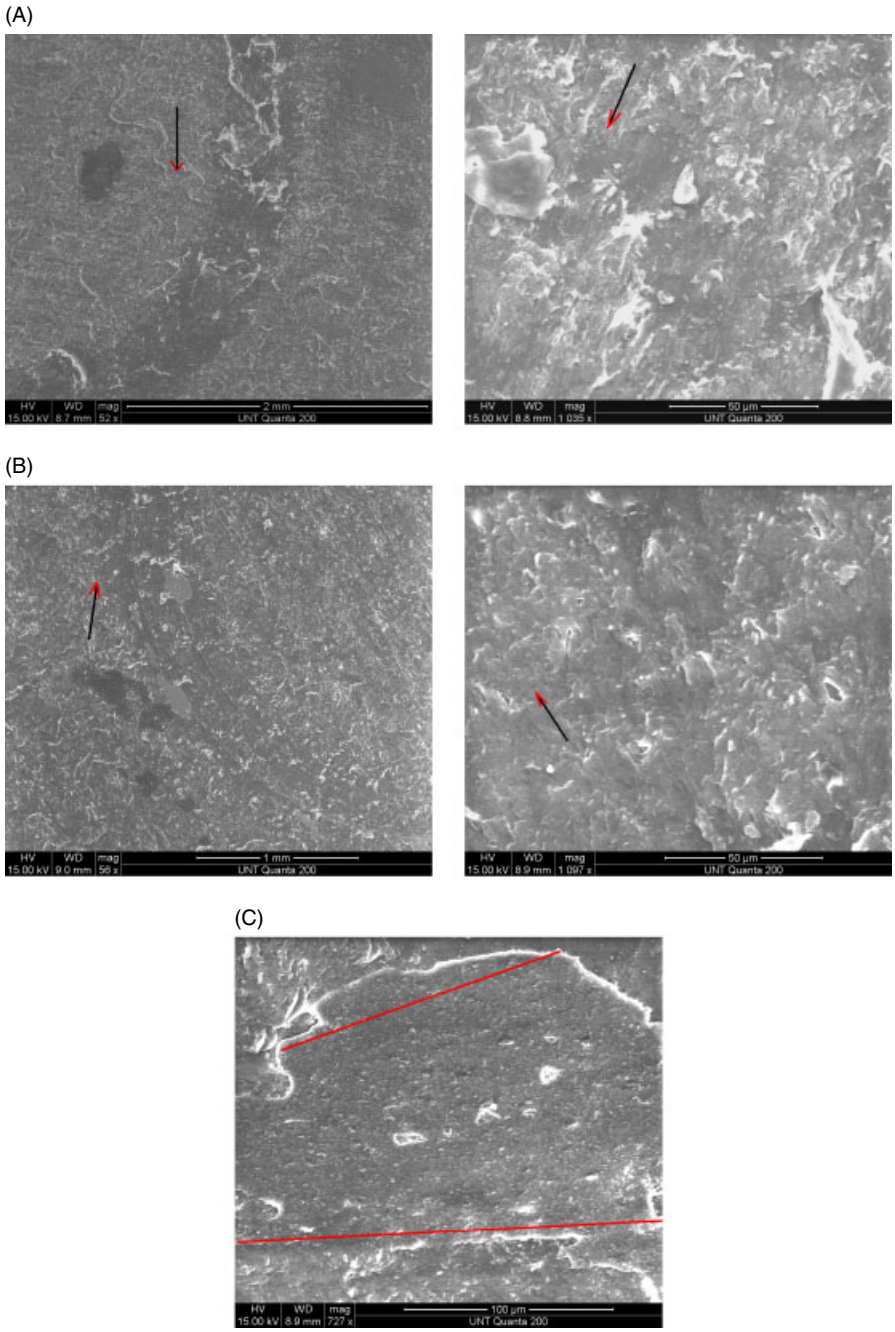

Figure 7. ESEM micrographs of wear track using steel ball: (A) TPV; (B) TPV + ceramic; (C) steel film inside wear track.

results can be explained in terms of matrix elasticity. As noted above, EPDM is a soft material; during friction testing it undergoes wear easily. EPDM provides more contacts of the filler to the ball while PP is stiff and cannot be depressed and worn out as easily.

Another important factor is heat generated during tribological testing. As expected, the sliding causes heat generation and increases the temperature of the contact surfaces. We have to remember that our polymers exhibit differences in their thermophysical properties such as thermal expansivity;[3] this should influence the tribological response of the samples. The amount of heat (Q) generated can be calculated as

$$Q = \mu P v \quad (1)$$

Here, μ is the dynamic friction, P the applied load in newtons and v the sliding speed in m s^{-1}. Values of Q obtained from Eqn (1) are expressed in joules and presented in Fig. 10 as a function of the Vickers hardness of the balls.

We find that the hardness of the balls has only a minor effect on heat generation during friction testing. PP composite maintains almost the same value of the heat for the entire hardness range, while heat generated for EPDM + ceramic increases with hardness, except for the highest hardness value. Overall, the highest heat value by far is found for EPDM + ceramic blend. Again, the softness of EPDM is important here. We recall the results seen in Figs 1 and 2: highest friction values for EPDM + ceramic result via Eqn (1) in high heat values. By the same token, lowest friction

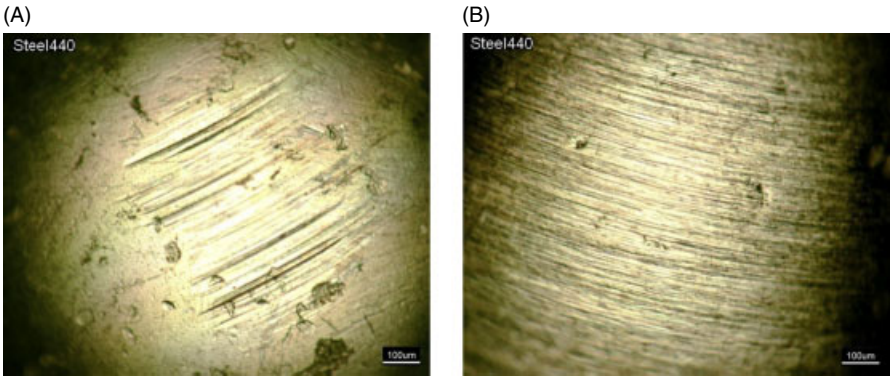

Figure 8. 440 steel ball surfaces after friction with (A) PP + ceramic and (B) EPDM + ceramic.

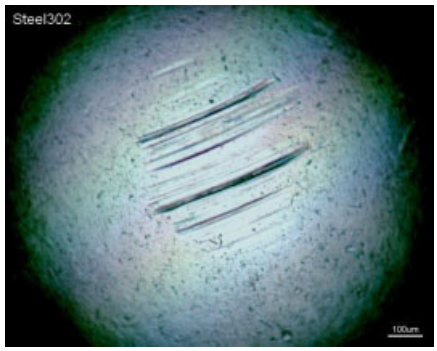

Figure 9. 302 steel ball surface after friction with TPV + ceramic at 1.0 N.

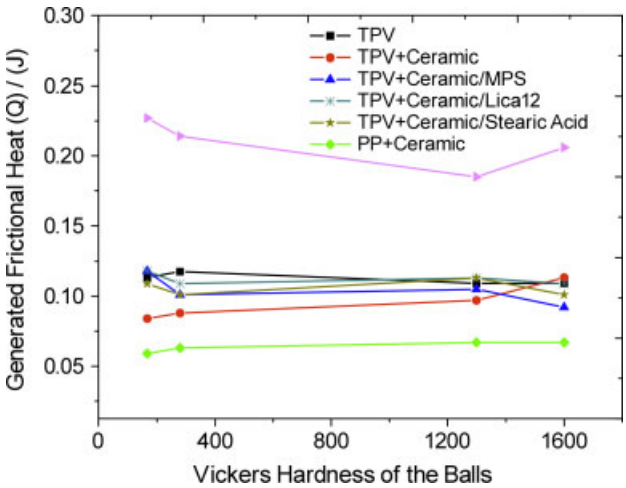

Figure 10. Heat generated as a function of Vickers hardness.

values for PP + ceramic against all partners result in the lowest heat generated.

The worn surfaces of the composites were analyzed using a profilometer. Figure 11 presents wear track cross-sections of the surface of TPV and TPV + ceramic blends (test conditions: load, 5.0 N; number of revolutions, 5000; speed, 100 rpm). The displaced areas are displayed in Fig. 12.

Compared to neat TPV, larger areas of wear tracks are seen for TPV + ceramic composites after friction with steel balls; however, a completely opposite tendency is observed after switching from a softer to a harder ball. As seen in Fig. 12, twice as large an area was removed from TPV during friction with WC and Si_3N_4. Higher wear of the TPV + ceramic on steel counter-surface can be related to the increased roughness of the ball due to abrasive wear during sliding tests. An uneven ball surface with deep, sharp scars on it apparently has a significant effect on material removal during dry friction. On the other hand, and as noted earlier, removed steel and possibly some ceramic particles act as third-body abrasives during the testing.

Cross-sectional areas so obtained were used to calculate the wear volume V_m as

$$V_m = 2\pi R_m A_m \tag{2}$$

Here, R_m and A_m represent the radius and the average cross-sectional area of the wear track, respectively. Then the wear rate Z in $mm^3\ N^{-1}\ m^{-1}$ was calculated as

$$Z = \frac{V_m}{WL} \tag{3}$$

Here, V_m is the volume loss of the sample after testing, W is the normal load and L is the length. The wear rates of the composites are shown in Fig. 13. We see that the wear rates increase somewhat with increasing Vickers hardness for each of our materials, but the increases are not dramatic. The lowest wear values are seen for PP + ceramic; we recall the lowest friction values in Figs 1 and 2 and also the lowest heat generated. The second lowest wear is for TPV + ceramic when no CAs are applied. This means that the ceramic protects against wear whether ceramic particles protrude from the surface or not.

CAs weaken somewhat the protective role of the ceramic filler. All wear curves for systems in which CAs are applied lie above the curves for PP + ceramic and TPV + ceramic systems. Consider now mechanical behavior. As reported in Brostow *et al.*,[3] addition of the ceramic increases the tensile modulus E; a further increase is achieved by application of CAs. There is a similar situation with the dynamic storage modulus E' at 1.0 Hz.[3] Thus, the use of the CAs enhances the mechanical properties but adversely affects the wear resistance. It might be interesting in the future to study such relationships in different types of composites – such as composites containing carbon nanotubes.[38,39] We note that one cannot generalize connections between wear and friction. Indentation and nanoidentation provide a different kind of tribological information,[40–42] while wetting angles for liquids on polymer surfaces provide a still different type of information.[43]

An important current activity consists of coating TE materials with polymers or reinforced polymers. We shall report results along these lines in future papers. The present results show that the type

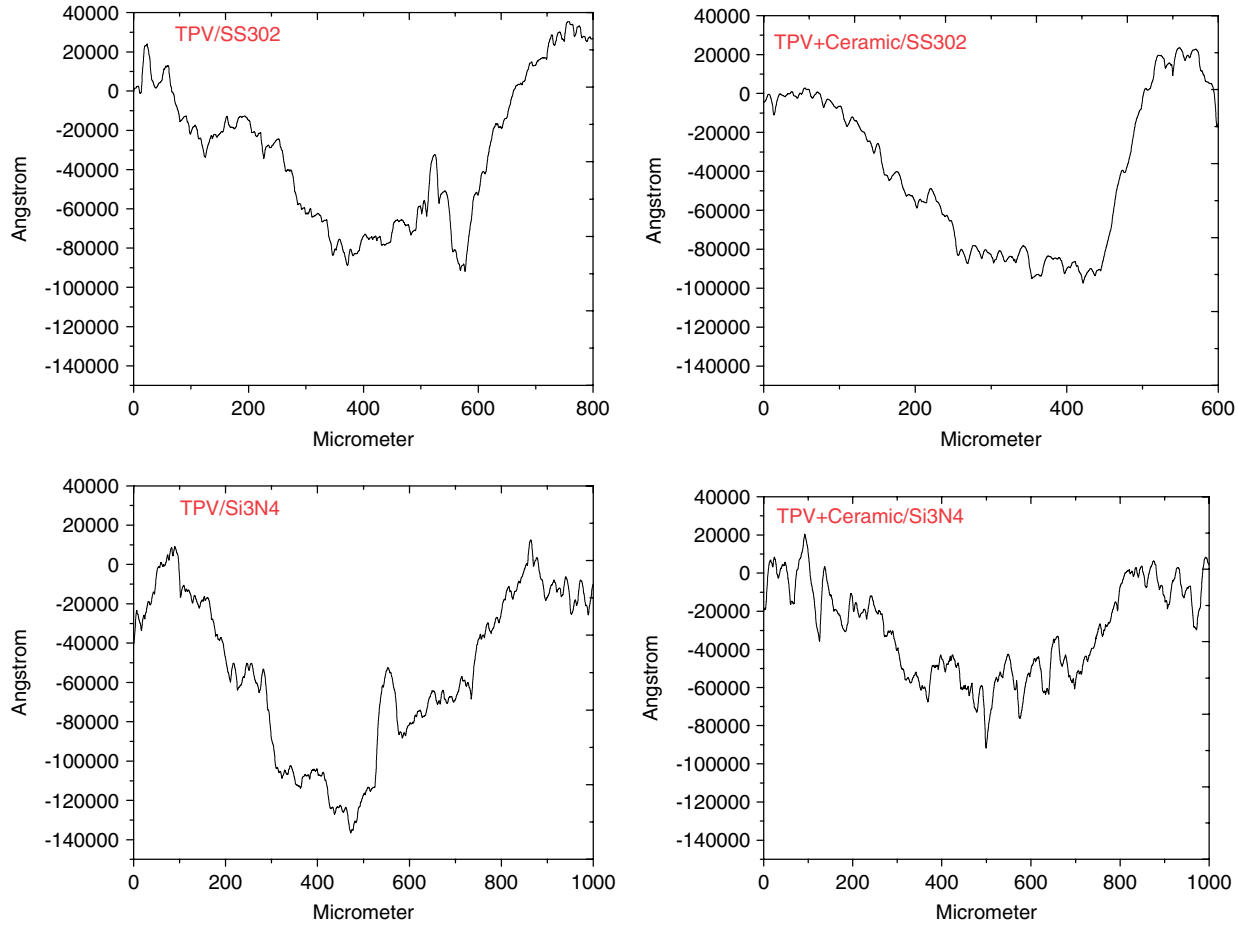

Figure 11. Cross-sections of wear tracks.

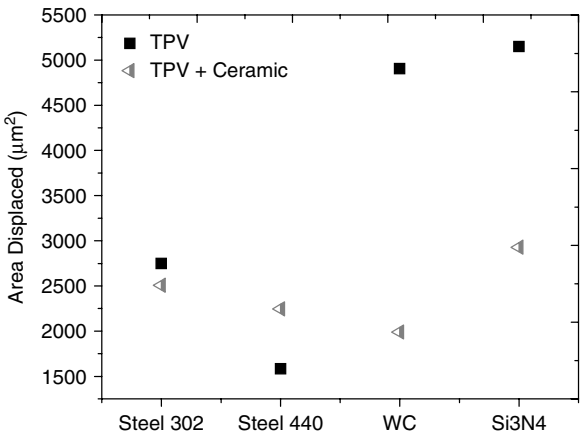

Figure 12. Area displaced.

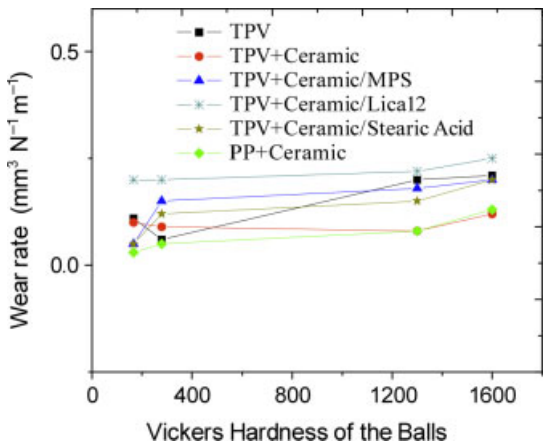

Figure 13. Wear rates.

of reinforcement and the treatment to which the reinforcement might be subjected can cause large differences in the performance of such coatings.

ACKNOWLEDGEMENTS

Partial financial support of this work by the II-VI Foundation, Bridgeville, PA, is gratefully acknowledged. We also appreciate discussions with John White, Marlow Industries Inc., Dallas, as well as comments on the manuscript by Prof. Rashmi C Desai, University of Toronto.

REFERENCES

1 Nolas GS, Sharp J and Goldsmid HJ, *Thermoelectrics: Basic Principles and New Materials Developments*. Springer, Berlin (2001).
2 Brostow W, Menard KP and White JB, *e-Polymers* 045 (2004).

3 Brostow W, Datashvili T, Geodakyan J and Lou J, *J Mater Sci* **46**:2445–2555 (2011).
4 Brostow W, Hagg Lobland HE and Narkis M, *J Mater Res* **21**:2422–2428 (2006).
5 Brostow W and Hagg Lobland HE, *Polym Eng Sci* **49**:1982–1985 (2008).
6 Brostow W, Datashvili T, McCarty R and White J, *Mater Chem Phys* **124**:371–376 (2010).
7 Brostow W, Hagg Lobland HE and Narkis M, *Polym Bull* **59**:1697–1707 (2011).
8 Carrión FJ, Espejo C, Sanes J and Bermudez MD, *Compos Sci Technol* **70**:2160–2167 (2010).
9 Brostow W, Chonkaew W and Menard KP, *Mater Res Innovat* **10**:389–393 (2006).
10 Bistac S, Galliano A and Schmitt M, *J Phys Condens Matter* **20**:354015 (2008).
11 Giraldo LF, Brostow W, Devaux E, Lopez BL and Perez LD, *J Nanosci Nanotechnol* **8**:3176–3183 (2008).
12 Carrión FJ, Sanes J and Bermúdez MD, *Mater Lett* **61**:4531–4535 (2007).
13 Bistac C, Schmitt M, Ghorbal A, Gnecco E and Meyer E, *Polymer* **49**:3780–3784 (2008).
14 Brostow W, Datashvili T and Huang B, *Polym Eng Sci* **48**:292–296 (2008).
15 Sanes J, Carrión JF, Jiménez AE and Bermúdez MD, *Tribol Lett* **21**:121–133 (2006).
16 Brostow W, Chonkaew W, Menard KP and Scharf T, *Mater Sci Eng A* **507**:241–251 (2009).
17 Sanes J, Carrión-Vilches JF and Bermúdez MD, *e-Polymers* 005 (2007).
18 Brostow W, Deborde J-L, Jaklewicz M and Olszynski P, *J Mater Educ* **24**:119–132 (2003).
19 Sanes J, Carrión FJ and Bermúdez MD, *Wear* **268**:1295–1302 (2010).
20 Bartenev GM and Lavrentev VV, *Friction and Wear of Polymers*. Elsevier, Amsterdam, pp. 230–235 (1981).
21 Roylance BJ, Williams JA and Dwyer-Joyce R, *Proc IMechE* **214J**:79–105 (2000).
22 Williams JA, *Tribol Int* **38**:863–870 (2005).
23 Hornbogen E, Friction and wear of materials with heterogeneous microstructure, in *Friction and Wear of Polymer Composites*, ed. by Friedrich K. Elsevier Science, New York, pp. 61–88 (1986).
24 Brostow W, Chonkaew W, Datashvili T and Menard KP, *J Nanosci Nanotechnol* **9**:1916–1922 (2009).
25 Myshkin NK, Petrokovets MI and Kovalev AV, *Tribol Int* **38**:910–921 (2005).
26 Barquins M, *Wear* **158**:87–117 (1992).
27 Zhang SW, *Tribology of Elastomers*. Elsevier Science, Amsterdam (2004).
28 Schweitz JÅ and Åhman L, Mild wear of rubber-based compounds, in *Friction and Wear of Polymer Composites*, ed. by Friedrich K. Elsevier Science, New York, pp. 289–327 (1986).
29 Bahadur S, *Wear* **245**:92–99 (2000).
30 Brostow W, Kovacevic V, Vrsaljko D and Whitworth J, *J Mater Educ* **32**:273–290 (2010).
31 Belon C, Chemtob A, Croutxé-Barghorn C, Rigolet S, Schmitt M, Bistac S, *et al*, *Polym Int* **59**:1175–1186 (2010).
32 Brostow W, Datashvili T and Hackenberg KP, *Polym Compos* **31**:1678–1691 (2010).
33 Brostow W, Cassidy PE, Macossay J, Pietkiewicz D and Venumbaka S, *Polym Int* **52**:1498–1505 (2003).
34 Desai RC and Kapral R, *Dynamics of Self-Organized and Self-Assembled Structures*. Cambridge University Press, Cambridge (2009).
35 Brostow W, Gorman BP and Olea-Mejia O, *Mater Lett* **61**:1333–1336 (2007).
36 Brostow W, Datashvili T, Strate GW and Lohse DJ, Ethylene–propylene–diene monomer elastomers, in *Polymer Data Handbook*, 2nd edition, ed. by Mark JE. Oxford University Press, New York, pp. 155–161 (2009).
37 Dec RT, Hryniewicz H and Komarek RK, Proceedings of the 30th Biennial Conference of the Institute for Briquetting and Agglomeration, Savannah, GA (2007).
38 Nogales A, Broza G, Roslaniec Z, Schulte K, Sics I, Hsiao BS, *et al*, *Macromolecules* **37**:7669–7672 (2004).
39 Broza G and Schulte K, *Polym Eng Sci* **48**:2033–2038 (2008).
40 Doerner MF and Nix WD, *J Mater Res* **1**:601–609 (1986).
41 Doerner MF, Gardner DS and Nix WD, *J Mater Res* **1**:845–851 (1986).
42 Beake BD, Bell GA, Brostow W and Chonkaew W, *Polym Int* **56**:773–778 (2007).
43 Kopczynska A and Ehrenstein GW, *J Mater Educ* **29**:325–340 (2007).

